Monoamide Derivatives of EDTA Incorporating Pendent Carboxylates or Pyridyls: Synthesis, Metal Binding, and Crystal Structure of a Dinuclear Ca^{2+} Complex Featuring Bridging Na^{+} Ions

Dr. Raminder S. Mulla,[(a)]* Dr. Javier Pitarch-Jarque,[(b)] Prof. Enrique García-España,[(b)]

Tanya Desa,[(c)] Dr. Elena Lurie-Luke,[(c)] and Prof. J. A. Gareth Williams[(a)]*

(a) Department of Chemistry, Durham University, Durham, DH1 3LE, U.K.

(b) Instituto de Ciencia Molecular (ICMol), Universidad de Valencia, C/ Catedrático José Beltrán, 2, 46980, Paterna, Valencia, Spain.

(c) Procter and Gamble Technical Centres Limited, Rusham Park, Whitehall Lane, Egham, Surrey, TW20 9NW.

Abstract

EDTA is a powerful, cheap and widely-used chelating unit for a large range of metal ions. To link it covalently to other molecules, the formation of an amide bond using one of the carboxylates is an attractive and simple approach, even though it may compromise metal ion binding as one of the four carboxylate donors is lost. Here we undertake a quantitative study of the metal ion binding of two new mono-amide derivatives of EDTA, namely **$AmGly_1$** and **$AmPy_1$**, featuring an additional coordinating carboxylate or pyridyl group in the amide, respectively. The compounds are conveniently synthesised through alkylation of the tris-*t*-butylester of ethylenediamine-triacetic acid with the appropriate α-chloroamide. The switch from carboxylate to amide is found to impact Fe^{3+} binding the most amongst the metal ions examined (Mg^{2+}, Ca^{2+}, Mn^{2+}, Fe^{3+}, Zn^{2+}), with a drop in log *K(ML)* of around 10 units in aqueous solution. The affinities for the other metals are less severely affected. Nevertheless, at the physiologically relevant pH of 7.4, their ability to bind Fe^{3+} is only reduced by around 6 log units when pFe^{3+} is considered (where [**L**]:[Fe^{3+}] = 10:1). **$AmGly_1$** forms a dinuclear Ca^{2+} complex which has been characterised crystallographically. It is a C_2-symmetric 2:2 complex featuring a dicapped octahedral coordination geometry around Ca^{2+}. In the crystal, the **$Ca_2(AmGly_1)_2$** units are linked via hydrated Na^{+} ions coordinated by a number of the oxygen atoms, including the pendent carboxylate.

* Corresponding author e-mails: r.s.mulla@durham.ac.uk j.a.g.williams@durham.ac.uk

Introduction

EDTA- type building blocks are used as metal-binding units in synthetic peptides,[1] nucleic acid affinity cleavage reagents[2–5] and monoclonal antibody-based radiopharmaceuticals.[6] In order to prepare **EDTA** derivatives that may then be conjugated to other molecules, four main strategies are used.[7] They are: (i) the incorporation of a reactive group on the ethylene diamine backbone of an **EDTA** derivative,[8] (ii) the incorporation of such a group into the methylene bridge,[9] (iii) using one of the carboxylate groups of **EDTA** to form an ester linkage, or (iv) using one of the carboxylates to form an amide linkage. These approaches are illustrated in ***Figure 1***. Each has different merits. The first two, although synthetically more laborious, afford building blocks which retain four carboxylate units to bind to the desired metal ions with affinities that are likely to be very close to those of **EDTA**. In contrast, the use of an ester or amide linkage can be less demanding synthetically, but may be expected to compromise the metal ion binding strength of the chelating unit.[10]

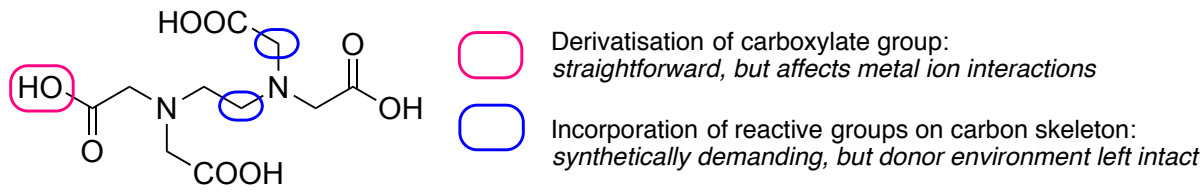

Figure 1. *Strategies for conjugating an EDTA unit to other molecules*

Even though the possibility of a loss in binding strength has been highlighted previously,[8,9] no studies have been published on interactions of the **EDTA** mono-amide motif with the metal ions most abundant in biological systems (i.e. Mg^{2+}, Ca^{2+}, Mn^{2+} and Zn^{2+}; and the trivalent Fe^{3+}). If binding data for **EDTA** mono-amides were to be collected and compared to those reported for **EDTA**, then the impact of the amide group on metal ion binding might be assessed. Moreover, the data may allow for some insight into *in vivo* speciation, and the favourability of transmetallation for systems incorporating **EDTA** mono-amide motifs.

To begin such an investigation then, we synthesised the novel ligands $\mathbf{AmGly_1}$, and $\mathbf{AmPy_1}$ (***Figure 2***) – which bear coordinating pendant groups – as easily characterisable models for

many of the more complex **EDTA** mono-amide structures (e.g. those conjugated to antibiotics, polypeptides and reactive functional groups) that are found in the literature and have been used as reagents in biological studies.[11–15] We then measured their protonation constants and binding constants to Mg^{2+}, Ca^{2+}, Mn^{2+}, Fe^{3+} and Zn^{2+} ions via potentiometry. Where possible, X-ray crystallography has been used to study the coordination chemistry of the metal complexes which these ligands form.

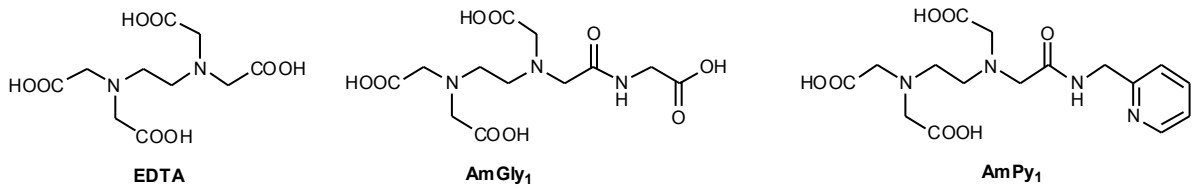

Figure 2. *The structures of the EDTA mono-amide derivatives* ***AmGly$_1$*** *and* ***AmPy$_1$****, which have been synthesised and characterised in this work, together with that of EDTA itself*

Results and Discussion

Ligand synthesis

In contrast to earlier syntheses of **EDTA** mono-amides reported in the literature, which often rely on amide coupling chemistry on the partially hydrolysed triethyl ester of **EDTA** or the partial reaction of the bis-anhydride of **EDTA**, we employed an amine alkylation strategy often used in the preparation of complexing agents for lanthanide ions. This enabled access to **AmGly$_1$** and **AmPy$_1$** by first using chloroacetyl chloride to prepare key electrophiles **1** and **2** (***Scheme 1***), which can then be used to alkylate triester **3** (***Scheme 2***). Because most of the intermediates along the route are relatively nonpolar and soluble in organic solvents, they can be prepared on a gram scale and are easily purified via typical laboratory techniques.

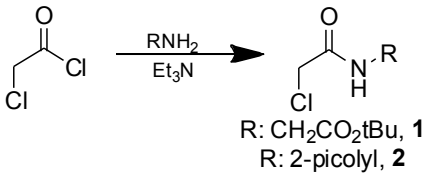

Scheme 1*. The synthesis of key electrophiles* ***1*** *and* ***2***

Initially, intermediate **3** was prepared via the route of Micklitsch,[16] in which N-benzylethylene diamine is alkylated using *t*-butyl bromoacetate and then debenzylated via catalytic hydrogenation, but it was found to be more convenient to use a statistical reaction between ethylenediamine and *t*-butyl bromoacetate, to access **3** in 20% yield in one step.[17] Although this approach gave lower yields, the faster access to **3** outweighed the disadvantage of the reduced yield.

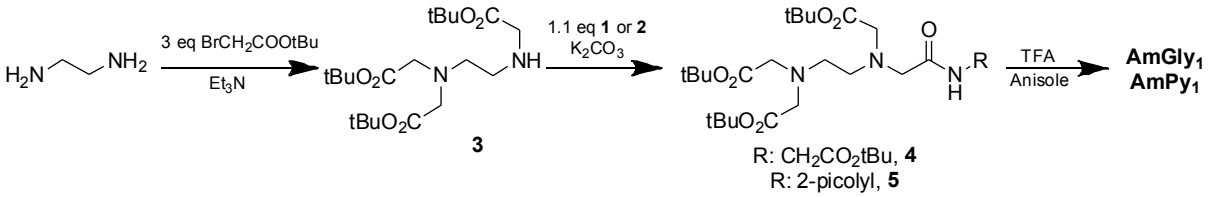

Scheme 2. *Synthesis of triester **3**, its alkylation using **1** or **2**, and subsequent deprotection to afford **AmGly$_1$** and **AmPy$_1$***

Alkylation of **3** to form **4** and **5**, followed by acid-mediated deprotection, thus afforded **AmGly$_1$** and **AmPy$_1$**. Product identity was confirmed via MS and NMR, whilst the homogeneity of the products was confirmed by HPLC.

Although combustion analysis was impracticable on these hygroscopic ligands, we were able to assess their extent of hydration prior to potentiometric analysis by the use of quantitative ^{1}H NMR to introduce a molecular weight correction. This correction was in turn verified by the satisfactory fitting of the experimental titration data.

Potentiometric measurements

Solutions for study were prepared at an ionic strength of 0.15 M using KCl and contained 1 mM of the analyte ligand. Four protonation constants were determined for both **AmGly$_1$** and **AmPy$_1$** (***Table 1***). The first protonation (log K = 9.76 and 9.44) is believed to be on a tertiary amine group for each ligand and the values are lower than those of **EDTA**, which we attribute to the inductive effect of the amide groups present, by analogy with earlier work on symmetrical **EDTA** bis-amides.[18]

Using UV-Vis spectroscopy to monitor the decrease in the absorbance of **AmPy$_1$** at 274 nm as a function of increasing pH, we were able to assign the second protonation of **AmPy$_1$** (log K = 5.42) as being on the pyridyl ring. Aside from this protonation constant, the other protonation constants for both **AmGly$_1$** and **AmPy$_1$** are quite similar, most likely because of the structural similarity between the two ligands.

Table 1. *Protonation constants[a] at 25°C, I = 0.15 M KCl, for **AmGly$_1$** and **AmPy$_1$**, with values for **EDTA**[b] included for comparison. Charges are omitted for clarity. Values in brackets (where appropriate) are the standard deviation in the last significant figure*

Species	log K[a](**AmGly$_1$**)	log K(**AmPy$_1$**)	log K(**EDTA**)[b]
HL	9.76 (1)	9.44 (7)	10.17
H_2L	4.69 (1)	5.42 (1)	6.11
H_3L	3.61 (1)	3.99 (7)	2.68
H_4L	2.27 (2)	2.13 (2)	2.0
H_5L	-	-	1.5

[a] $K = [H^{n+1}L] / [H] [H^nL]$
[b] Data from Martell and Smith[19] at T = 25°C and I = 0.1M.

Both $AmGly_1$ and $AmPy_1$ form stable complexes at alkaline pH with Ca^{2+}, Mg^{2+}, Fe^{3+}, Mn^{2+} and Zn^{2+}. Distribution diagrams for the complexes formed have been provided in ***Figures S1-4*** of the Supporting Information.

For both **AmGly$_1$** and **AmPy$_1$**, the most stable complex formed was that of Fe^{3+}, consistent with the relative hardness of the donor set. The difference between metal ion affinities for Zn^{2+} and Fe^{3+} that **AmGly$_1$** shows is notable, since it is unusually small compared to classical aminocarboxylate ligands like **EDTA** and **DTPA**, which show a separation of 5–10 log units between their Zn^{2+} and Fe^{3+} affinities to the fully deprotonated ligand.[19] When the metal–ligand stability constants of the deprotonated "**L**" forms of **AmGly$_1$** and **AmPy$_1$** are compared to those of **EDTA**, a reduction of 2 to 3 log units is seen for binding to Ca^{2+}, Mg^{2+}, Mn^{2+} and Zn^{2+}, due to one less carboxylate group being present in **AmGly$_1$** and **AmPy$_1$**.

For Fe^{3+}, a much more marked destabilisation of about 10 log units is noted, presumably due to the especially hard character of Fe^{3+} being more suited to the tetra-carboxylate donor set of **EDTA**. Indeed, these differences demonstrate the profound impact that small changes in the donor set of a ligand can have on metal ion affinity and selectivity.[20]

The low *K* (MH_{-1}**L**) values of 3.91 and 4.0 measured for the Fe^{3+} complexes of **AmGly$_1$** and **AmPy$_1$** also warrants comment, and may be due to deprotonation of their amide groups leading to N- instead of O- coordination of the amide groups to Fe^{3+}; a coordination mode proposed by Martell[21] for the Fe^{3+} complex of the symmetrical bis-amide analogue of **AmGly$_1$**.

Table 2. *Formation constants at 25°C, I = 0.15 M KCl for metal ion complexes of* ***AmGly$_1$*** *and* ***AmPy$_1$.*** *Values in brackets (where appropriate) are the standard deviation in the last significant figure*

Equilibrium [a]	Ca^{2+}	Mg^{2+}	Fe^{3+}	Mn^{2+}	Zn^{2+}
			AmGly$_1$		
log *K* (**MHL**) [b]	4.19 (3)	5.6 (1)	3.06 (1)	3.61 (2)	3.49 (2)
log *K* (**ML**) [c]	9.31(2)	6.63 (4)	15.27 (5)	11.97 (1)	14.11 (3)
log *K* (MH_{-1}**L**) [d]	11.6 (1)	-	3.91 (8)	11.44 (6)	10.17 (9)
			AmPy$_1$		
log *K* (**MHL**)	4.75 (4)	-	3.82 (2)	4.86 (2)	4.65 (5)
log *K* (**ML**)	8.71 (3)	5.84 (2)	15.3 (1)	10.99 (2)	13.67 (9)
log *K* (MH_{-1}**L**)	-	-	4.0 (1)	10.85 (4)	8.9 (2)
			EDTA[e]		
log *K* (**MHL**)	-	-	-	3.1	3.0
log *K* (**ML**)	10.61	8.83	25.0	13.81	16.44

[a] Charges have been omitted for clarity.

[b] K (MHL) = [MHL]/[ML][H]

[c] K(ML) = [ML]/[M][L]

[d] K ($MH_{-1}L$) = [ML]/[MH_{-1}L][H], either due to metal ion hydrolysis, or amide deprotonation.

[e] Data from Martell and Smith[19] at T=25ºC and I=0.1M.

pM^{n+} calculations

So as to enable cross comparison of the effect of the pendent groups on metal ion binding between **$AmGly_1$** and **$AmPy_1$**, pM^{n+} values (where $pM^{n+} = -\log[M^{n+}_{free}]$) were calculated from our potentiometric titration data using the HySS[22] software (***Table 3***) and compared to those obtained for **EDTA** under the same simulated conditions, in which a ligand to metal ratio of 10 to 1 is used.[23] By comparing the extent of metal ion sequestration in this way, the protonation states of each ligand could be accounted for, giving a better indication of how extensively **$AmGly_1$** and **$AmPy_1$** sequester the metal ions under study at physiological pH.

It is interesting to note that at pH 7.4, although the pM^{n+} values for **EDTA** are all higher than those of the **EDTA** mono-amides, the values of pFe^{3+} for the mono-amide ligands are only 6 log units less than that of **EDTA**, which would not be expected from a simple comparison of the Fe^{3+}-ligand binding data for the "**L**" form of either ligand, and so not accounting for their basicities.

Table 3. *$p[M^{n+}]$ values at pH 7.4 at 25°C, I = 0.15M KCl for **$AmGly_1$** and **$AmPy_1$**. [**L**] = 10 μmol dm^{-3} and $[M^{n+}]$ = 1 μmol dm^{-3}*

Species	**$AmGly_1$**	**$AmPy_1$**	**EDTA**
Ca^{2+}	7.9	7.6	8.8
Mg^{2+}	6.1	6.0	7.0
Fe^{3+}	17.4	17.6	23.2
Mn^{2+}	10.6	9.9	12.0
Zn^{2+}	12.7	12.6	14.6

It can be seen from the pM^{n+} values that, with the exception of Fe^{3+}, **$AmGly_1$** has slightly higher metal ion affinities than **$AmPy_1$** but the difference in pendent groups does not appear to have a *marked* effect on the extent of metal ion sequestration around physiological pH.

These data are the first quantitative indication of the extent to which metal ion affinities are impacted when a carboxylate group is exchanged for an amide in **EDTA** type fragments, and so may enable a critical evaluation of their use in the design of the systems mentioned earlier.

Structures of AmGly$_1$ in the solid state

We were able to obtain crystal structures of **AmGly$_1$** in the free state, and as its Ca^{2+} complex. The crystallographic data are given in ***Table S1*** of the Supporting Information. Free **AmGly$_1$** crystallised as its zwitterion from aqueous solution at pH=2, after slow evaporation. The ligand crystallises in space group $P2_1/c$, and displays moderately strong hydrogen bonding between proton H2 and carboxylate oxygen O8 (2.044 Å, ***Figure 3***). Another hydrogen bond, of length 1.996 Å, is present between H3 and amide oxygen O3. These hydrogen atoms are on the tertiary amine groups of **AmGly$_1$** and the H2–O8 distance is the shorter of the two.

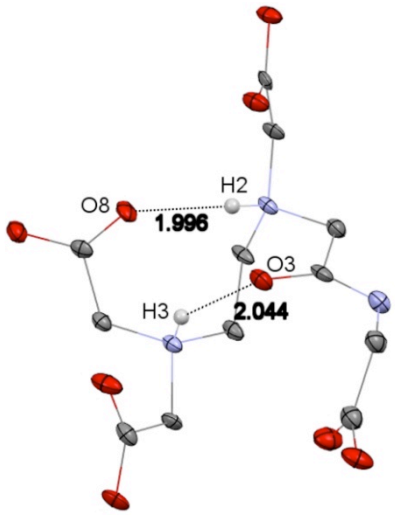

Figure 3. *Molecular structure in the crystal of the **AmGly$_1$** ligand. Hydrogen bond distances are in Å. Thermal ellipsoids are shown at the 50% probability level*

A Ca^{2+} complex of **AmGly$_1$**, **Ca$_2$(AmGly$_1$)$_2$** (molecular formula: (4[Na_3Ca(**H$_{-4}$AmGly$_1$**)$(H_2O)_6$] 4Cl•$3H_2O)_3 \cdot H_2O$), ***Figure 4***), was obtained through slow evaporation of a basified solution of $CaCl_2$ and **AmGly$_1$**. This 2 : 2, C_2-symmetric binuclear complex possesses a dicapped octahedral coordination geometry about the Ca^{2+} ions, both of which are 8-coordinate. The coordination set of each Ca^{2+} ion is identical, and consists of two tertiary amines, the amide oxygen and three carboxyl oxygens, all of which are from a single **AmGly$_1$** unit. Each **AmGly$_1$** ligand also possesses a μ–carboxylate donor which coordinates to both Ca^{2+} ions in the complex, leading to a Ca–Ca distance of 3.778(1) Å, which is similar to other binuclear Ca^{2+} complexes containing bridging carboxyl donors.[24,25] Both Ca^{2+} ions are also coordinated by one water molecule which completes the coordination sphere.

The bond distances and bite angles (***Table 4***) for the chelate rings in **Ca$_2$(AmGly$_1$)$_2$** are also comparable to those found in eight-coordinate Ca^{2+} complexes with similar donor sets.[26–29]

Furthermore, it can be seen that the pendent carboxylate group does not coordinate to either Ca^{2+} ion in the dimer.

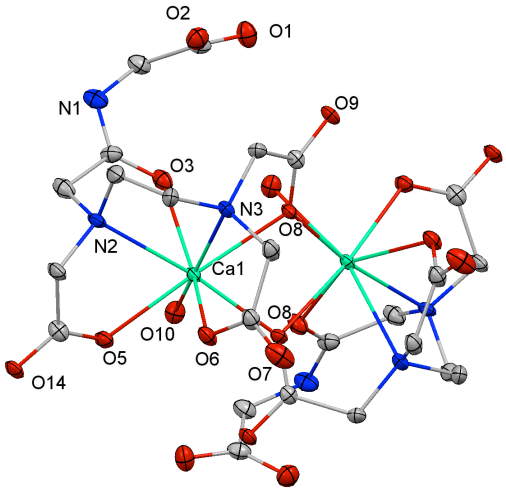

Figure 4. *A simplified view (omitting H atoms, Na^+ cations, associated water molecules and Cl^- ions) of the binuclear* ***$Ca_2(AmGly_1)_2$*** *complex, illustrating the coordination environment around the Ca^{2+} atoms, which are shown in cyan. Thermal ellipsoids are shown at the 50% probability level*

Table 4. *Selected bond distances (Å) and angles (°) for* ***$Ca_2(AmGly_1)_2$***

Bond distances		**Bond angles**	
Bond	Distance / Å	Atoms	Angle /°
Ca1—O8^{i}	2.341 (3)	N2—Ca1—N3	69.60 (11)
Ca1—O8	2.447 (3)	O3—Ca1—N2	67.24 (10)
Ca1—O3	2.420 (3)	O5—Ca1—N2	67.63 (10)
Ca1—O10	2.524 (3)	O3—Ca1—N3	91.52 (10)
Ca1—O6	2.422 (3)	O5—Ca1—O8	174.05 (9)
Ca1—O5	2.351 (3)	O5—Ca1—O10	70.93 (9)
Ca1—N3	2.599 (3)	O8—Ca1—N3	63.15 (9)
Ca1—N2	2.577 (3)	O8^{i}—Ca1—O8	68.72 (11)

(i) −x+3/2, *y*, −z+1/2;

Although the contacts are not shown in ***Figure 4***, the oxygens coordinated to the Ca^{2+} ions in the dimeric unit, i.e. O1, O2, O5, O9, O14 and the water oxygen, O10, also coordinate to Na^+ ions, which are in turn hydrated by either one or two water molecules, depending on the relative positions of the Na^+ ions in the chain. These six Na^+ ions serve to separate individual **$Ca_2(AmGly_1)_2$** units to give an A-B-A-B- type structure in the individual chains, which are in turn linked to one another by N-H···Cl^- and H-O-H···Cl^- hydrogen bonding interactions

(

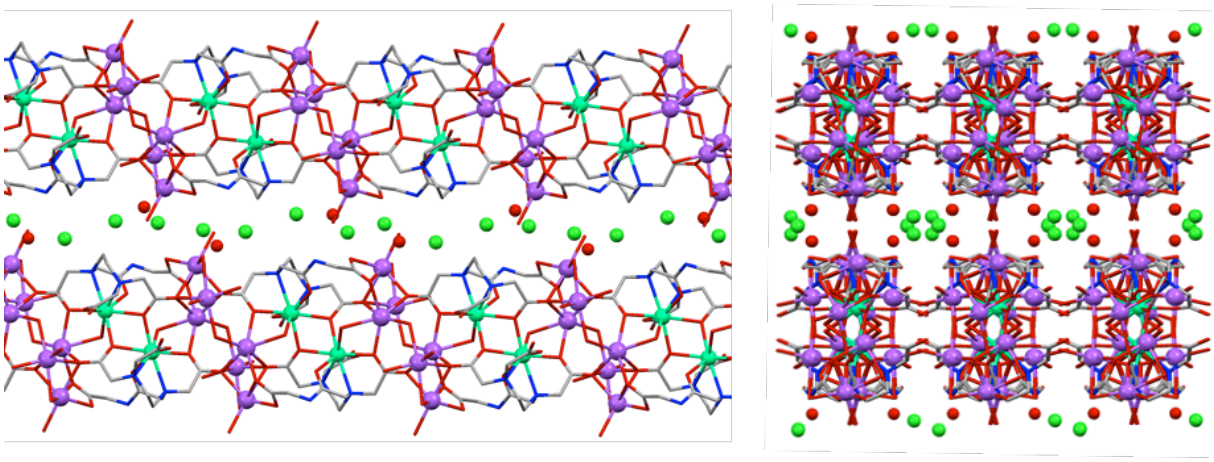

Figure 5).

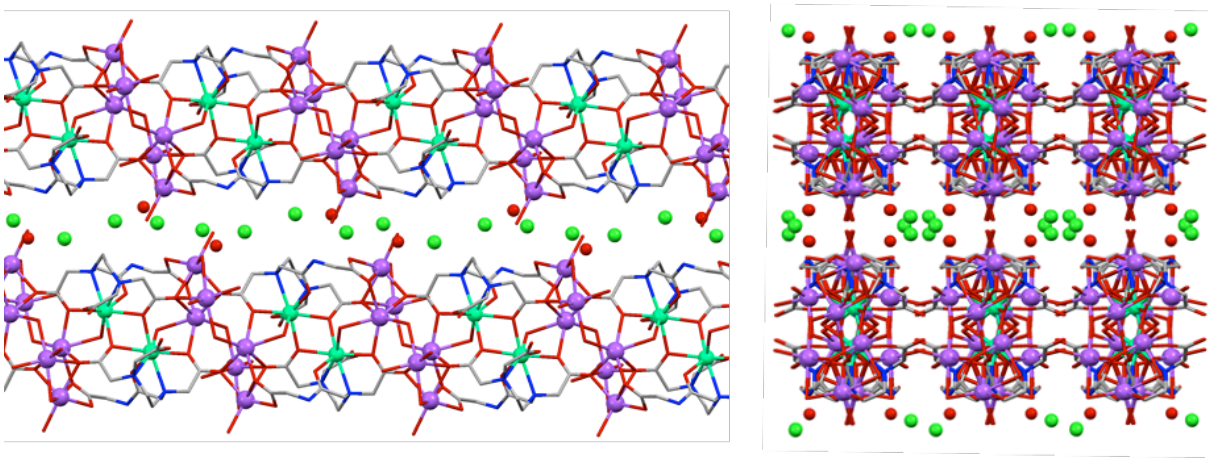

Figure 5. *Lateral (left) and upright (right) views of the polymeric structure of* ***$Ca_2(AmGly_1)_2$*** *showing the bridging Na^+ ions between each dimeric unit (purple) and Cl^- ions between individual chains (green). All of the metal ions, Cl^- ions and non-coordinating water molecules have been shown as spheres to emphasise their location in the structure*

As a complement to the work of Ulvenlund *et al.*, who showed that hydrogen bonding interactions between **EDTA** amides bearing pendent uracil moieties could allow the formation of linear tape-like structures,[30] our results show that interactions between the peripheral groups on ligands like **$AmGly_1$** and cations are an alternative strategy for the generation of supramolecular systems based on amides of **EDTA**, and that these groups can be incorporated without perturbing the coordination of the central metal ion.

Conclusions

The novel ligands **AmGly$_1$** and **AmPy$_1$** have been synthesised and their metal ion binding behaviours to a selection of biologically relevant metal ions (Ca^{2+}, Mg^{2+}, Mn^{2+}, Fe^{3+} and Zn^{2+}) have been characterised via pH potentiometry and X-ray crystallography. The metal ion affinities for the ligands are highest for Fe^{3+}, with both ligands forming similarly stable chelates to the above ions at physiological pH.

It is apparent that **AmGly$_1$** and **AmPy$_1$** form less stable complexes (by about 2 to 3 log units) to Ca^{2+}, Mg^{2+}, Mn^{2+} and Zn^{2+} than does **EDTA**, and that changing one carboxylate group to an amide causes a dramatic decrease (about 10 log units) in Fe^{3+}–**L** complex stability (**L**= **AmGly$_1$** and **AmPy$_1$**) compared to **EDTA**. However, at pH 7.4, the pFe^{3+} values of the monoamide derivatives are only about 6 log units lower than for **EDTA**.

We also conclude that changing the pendant group on these **EDTA**-monoamide ligands does not have a large effect on metal ion affinity. Crystallisation of **AmGly$_1$** at high pH leads to a coordination polymer, with binuclear **Ca$_2$(AmGly$_1$)$_2$** complexes being bridged by hydrated sodium cations forming the repeat unit. This may, in turn, be a strategy from which other coordination polymers incorporating metal complexes of **EDTA** amides, can be generated.

Supporting Information Summary

Details of experimental procedures; titrimetric studies and speciation diagrams; synthetic procedures; characterisation data for new compounds; ^{1}H and ^{13}C NMR spectra.

Acknowledgements RSM and JAGW are grateful to Procter and Gamble for financial support, whilst JPJ and EGE thank the Spanish MINECO, E.U. FEDER funds (CTQ2013-14892, CONSOLIDER INGENIO 2010-CSD2010-00065, Unidad de Excelencia MDM 2015-0538) and Generalitat Valenciana (PROMETEO II 2015-002).

Keywords

Azacarboxylate ligands; crystal structure; dinuclear calcium complex; EDTA; metal binding constants.

References

[1] T. M. Rana, M. Ban, J. E. Hearst, *Tetrahedron Lett.* **1992**, *33*, 4521–4524.

[2] H. E. Moser, P. B. Dervan, *Science* **1987**, *238*, 645–650.

[3] P. E. Floreancig, S. E. Swalley, J. W. Trauger, P. B. Dervan, *J. Am. Chem. Soc.* **2000**, *122*, 6342–6350.

[4] J. C. Joyner, J. A. Cowan, *J. Am. Chem. Soc.* **2011**, *133*, 9912–9922.

[5] J. C. Joyner, L. Hocharoen, J. A. Cowan, *J. Am. Chem. Soc.* **2012**, *134*, 3396–3410.

[6] D. A. Westerberg, P. L. Carney, P. E. Rogers, S. J. Kline, D. K. Johnson, *J. Med. Chem.* **1989**, *32*, 236–243.

[7] L. Lattuada, A. Barge, G. Cravotto, G. B. Giovenzana, L. Tei, *Chem. Soc. Rev.* **2011**, *40*, 3019–3049.

[8] M. W. Brechbiel, O. A. Gansow, R. W. Atcher, J. Schlom, J. Esteban, D. Simpson, D. Colcher, *Inorg. Chem.* **1986**, *25*, 2772–2781.

[9] J. F. W. Keana, J. S. Mann, *J. Org. Chem.* **1990**, *55*, 2868–2871.

[10] C. F. Meares, T. G. Wensel, *Acc. Chem. Res.* **1984**, *17*, 202–209.

[11] A. Leonov, B. Voigt, F. Rodriguez-Castañeda, P. Sakhaii, C. Griesinger, *Chem. - Eur. J.* **2005**, *11*, 3342–3348.

[12] I. E. Platis, M. R. Ermacora, R. O. Fox, *Biochemistry (Mosc.)* **1993**, *32*, 12761–12767.

[13] K. Shin, Y. Dae-Hawn, *J KorChem Soc* **1999**, *43*, 611–613.

[14] C. M. Micklitsch, P. J. Knerr, M. C. Branco, R. Nagarkar, D. J. Pochan, J. P. Schneider, *Angew. Chem. Int. Ed.* **2011**, *50*, 1577–1579.

[15] D. L. Boger, J. Zhou, *J. Org. Chem.* **1993**, *58*, 3018–3024.

[16] C. M. Micklitsch, Q. Yu, J. P. Schneider, *Tetrahedron Lett.* **2006**, *47*, 6277–6280.

[17] T. Storr, B. R. Cameron, R. A. Gossage, H. Yee, R. T. Skerlj, M. C. Darkes, S. P. Fricker, G. J. Bridger, N. A. Davies, M. T. Wilson, et al., *Eur. J. Inorg. Chem.* **2005**, *2005*, 2685–2697.

[18] A. F. Danil de Namor, D. Alfredo Pacheco Tanaka, *J. Chem. Soc. Faraday Trans.* **1998**, *94*, 3105–3110.

[19] R. M. Smith, A. E. Martell, *Critical Stability Constants*, Springer US : Imprint : Springer, Boston, MA, **1989**, pp 204–211.

[20] R. D. Hancock, A. E. Martell, *Chem. Rev.* **1989**, *89*, 1875–1914.

[21] R. J. Motekaitis, A. E. Martell, *J. Am. Chem. Soc.* **1970**, *92*, 4223–4230.

[22] L. Alderighi, P. Gans, A. Ienco, D. Peters, A. Sabatini, A. Vacca, *Coord. Chem. Rev.* **1999**, *184*, 311–318.

[23] W. R. Harris, K. N. Raymond, F. L. Weitl, *J. Am. Chem. Soc.* **1981**, *103*, 2667–2675.

[24] L. A. Clapp, C. J. Siddons, D. G. VanDerveer, J. H. Reibenspies, S. B. Jones, R. D. Hancock, *Dalton Trans.* **2006**, 2001–2007.

[25] B. L. Barnett, V. A. Uchtman, *Inorg. Chem.* **1979**, *18*, 2674–2678.

[26] B. Metz, D. Moras, R. Weiss, *Acta Crystallogr. B* **1973**, *29*, 1377–1381.

[27] J. D. Owen, *J. Chem. Soc. Dalton Trans.* **1978**, 1418–1423.

[28] L. A. Clapp, C. J. Siddons, J. R. Whitehead, D. G. VanDerveer, R. D. Rogers, S. T. Griffin, S. B. Jones, R. D. Hancock, *Inorg. Chem.* **2005**, *44*, 8495–502.

[29] W. Tong, R. Zhang, T. Zhang, L. Yang, *RSC Adv.* **2015**, *5*, 22031–22037.

[30] S. Ulvenlund, A. S. Georgopoulou, D. M. P. Mingos, I. Baxter, S. E. Lawrence, A. J. P. White, D. J. Williams, *J. Chem. Soc. Dalton Trans.* **1998**, 1869–1878.

Table of Contents Entry

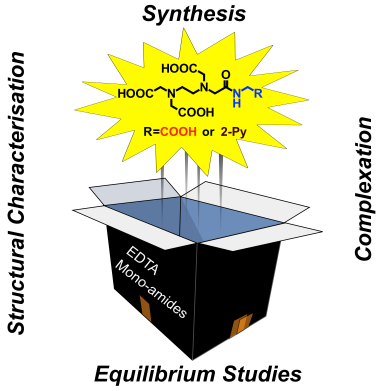

The synthesis and metal ion complexation properties of two novel EDTA-based mono-amide ligands, bearing additional potentially ligating groups (CO_2H or pyridyl), are reported and discussed. They display a marked reduction in metal ion affinity compared to EDTA (for Ca^{2+}, Mg^{2+}, Fe^{3+}, Mn^{2+} or Zn^{2+}). The Ca^{2+} complex of the ligand bearing the pendent carboxylate forms an extended polymeric structure featuring bridging Na^{+} ions, an unprecedented structural form for EDTA amide derivatives.